Journal of Soil Science and Plant Nutrition
https://doi.org/10.1007/s42729-025-02940-9

ORIGINAL PAPER

CO_2 and N_2O Emissions after Digestate Application Responded Differently to Topsoil Dilution and Soil Erosion State

Ayten Pehlivan[1,2] · Mathias Hoffmann[1] · Matthias Lück[1] · Steffen Kolb[1,2] · Michael Sommer[1] · Jürgen Augustin[1] · Maren Dubbert[1] · Maire Holz[1]

Received: 5 June 2025 / Accepted: 17 December 2025

Abstract
The application of digestates supports soil fertility by restoring soil organic matter (SOM) and supplying nitrogen (N). However, their application can increase greenhouse gas (GHG) emissions from agriculture. Targeted digestate application to soils where erosion has mixed subsoil into topsoil may reduce emissions, as the lower SOM saturation in this diluted topsoil could enhance stabilization of organic inputs. This study investigates whether topsoil dilution through erosion can reduce carbon dioxide (CO_2) and nitrous oxide (N_2O) emissions following digestate application. We conducted an incubation experiment simulating erosion-induced topsoil dilution. Three different soils from Uckermark region, Germany—non-eroded (LL), moderately eroded (eLL), and strongly eroded (RZ)—were incubated for 26 days in an automated gas exchange system. Topsoil was diluted with 20% subsoil, and digestate applied as organic fertilizer. CO_2 and N_2O emissions were measured; undiluted, unfertilized soils served as controls. Digestate increased CO_2 and significantly raised N_2O emissions in all soils. Topsoil dilution reduced CO_2 emissions in LL and showed similar trends in eLL and RZ, though the effect weakened with erosion severity, likely due to existing C-undersaturation in these soils. N_2O responses varied: emissions decreased in eLL (high clay and reactive mineral content), possibly due to enhanced N stabilization, but increased in RZ (calcareous, high-pH soil likely promoting nitrification) and slightly in LL, possibly due to lowered carbon-to-nitrogen (C: N) ratio. Topsoil dilution can mitigate digestate-induced CO_2 but may elevate N_2O emissions depending on soil properties. Therefore, site-specific management is key to lowering GHGs in erosion-prone soils.

Keywords Nitrous oxide · Carbon dioxide · Erosion · Topsoil dilution · Digestate fertilization

1 Introduction

The use of organic fertilizers is an essential farming practice for maintaining the fertility of arable soils. It facilitates the restoration and maintenance of soil organic matter (SOM) and the supply of plant nutrients, such as nitrogen (N) (Diacono and Montemurro 2011; Larney and Angers 2012). However, the risk of environmental pollution is higher with organic N fertilizers than with synthetic ones in case of improper use, such as application to the soil surface or outside the growing season (Rashmi et al. 2020; Zhang et al. 2012). What is currently important is its contribution to the increased role of arable land as a source of climate-relevant greenhouse gases (GHG), including nitrous oxide (N_2O) and carbon dioxide (CO_2) (Loubet et al. 2011; Möller 2015; Smith et al. 2008). This seems to be particularly true for digestate, a nutrient-rich byproduct produced in ever-increasing quantities worldwide when biogas is extracted from plant waste or organic fertilizer (Möller et al. 2015; O'Connor et al. 2022; Revuelta-Aramburu et al. 2025). Compared to other organic fertilizers, such as slurry, digestate contains higher levels of volatile ammonium nitrogen (NH_4^+-N), has a higher pH value, and contains a lower proportion of organic carbon (OC) compounds (Jäger et al. 2013; Möller et al. 2015; Nkoa 2014; Zhang et al. 2024). There are various indications that this is associated with a higher potential for ammonia (NH_3) volatilization and

✉ Ayten Pehlivan
Ayten.Pehlivan@zalf.de

[1] Leibniz Centre for Agricultural Landscape Research, Eberswalder Straße 84, Müncheberg 15374, Germany

[2] Thaer-Institute of Agricultural and Horticultural Sciences, Humboldt-Universität zu Berlin, Invalidenstraße 42, Berlin 10099, Germany

Published online: 20 January 2026

N_2O and CO_2 emissions after application to fields than with other organic or synthetic N fertilizers (Johansen et al. 2013; Rosace et al. 2020). In some cases, extremely high N_2O emissions following digestate application have been observed (Dietrich et al. 2020; Ma et al. 2011; Wang et al. 2014).

An option for mitigating the environmental and climate impact of digestate and other organic fertilizers is their preferential application to soils where carbon (C) and nutrient-poor subsoil has recently been mixed into the topsoil. This topsoil dilution is very often the result of soil erosion (Gregorich et al. 1998; Pehlivan et al. 2025; Pennock 1998; Vaidya et al. 2024; Zentgraf et al. 2024) and typically occurs on the slopes of hilly farmland in the aftermath of erosion events. In particular, plowing after an erosion event mixes the subsoil into the reduced topsoil layer (Gerke and Hierold 2012; Sommer et al. 2008). Consequently, the amount of nutrients and organic soil carbon (SOC) also decreases significantly. This usually leads to soil C undersaturation (Hassink 1997; Stewart et al. 2007; Xiao et al. 2018). This again increases the soil's ability to stabilize C by accumulating OC in the form of microbial necromass or mineral-associated organic matter (MAOM) (Doetterl et al. 2025; Georgiou et al. 2025). In other words, erosion-induced topsoil dilution induces a temporary increase in the accumulation of assimilate C in the diluted topsoil until the original SOC content and stock is restored, a phenomenon also referred to as "dynamic replacement" (Dialynas et al. 2017; Doetterl et al. 2016; Harden et al. 1999; Larney et al. 2016; Remus et al. 2018). While many details are still unclear, this process is apparently linked to reduced mineralization of OC and thus reduced CO_2 emissions, potentially resulting in a net CO_2-C sink on eroded soils (Doetterl et al. 2016; Hoffmann et al. 2017, 2018; Lal 2019; Vaidya et al. 2021). However, it remains unclear whether this CO_2-C sink function, which is associated with reduced CO_2 emissions from eroded soils, also operates in the context of digestate application (Levavasseur et al. 2022; Reuland et al. 2022).

Because of the close link between the C and N cycles, it is reasonable to assume that erosion-induced topsoil dilution leads to N undersaturation as well. This should result in increased temporary immobilization or stabilization of N in the form of the accumulation of organic N compounds in the soil (Bingham and Cotrufo 2016; Castellano et al. 2012; Knicker 2011; van Groenigen et al. 2015). So far, there is very little concrete information if this really takes place. However, a model experiment by Schoof et al. (2025) have shown that erosion-induced dilution of topsoil can lead to reduced gross N mineralization and N_2O emissions. Yet, it remains unclear if the NH_4^+-N applied with digestate behaves the same way in the soil. In other words, the question is whether it is also subject to increased immobilization, stabilization, and reduced N_2O emission.

On eroded slopes, however, there is a small-scale sequence of soils with different erosion states. The closer the original C-horizon (parent material) is to the soil surface because of soil erosion, the greater the erosion state. Depending on erosion state, the topsoil is diluted with subsoil material of very different chemical-physical composition (Doetterl et al. 2025; Gerke and Hierold 2012; Gerke et al. 2016; Sommer et al. 2008, 2016). There is now some evidence that the erosion state that a soil type exhibits can have a strong impact on CO_2 and N_2O emissions (Holz and Augustin 2021; Vaidya et al. 2023, 2024). In addition, high small-scale variability in N_2O emissions at erosion sites has been linked to the distribution of different erosion states in the soil (Gu et al. 2011; Vaidya et al. 2023; Vilain et al. 2010).

To address these knowledge gaps, this study focuses on understanding the role of erosion status and digestate fertilization in shaping GHG dynamics and nutrient retention under controlled conditions. We compared three soil types representing increasing erosion states: non-eroded Luvisol (LL), eroded Luvisol (eLL), and strongly eroded Calcaric Regosol (RZ), from the hummocky, north-eastern German young moraine landscape characterised by varying degrees of erosion over short distances. To assess the effects of erosion-induced topsoil dilution on CO_2 and N_2O emissions, we incubated the soils under controlled conditions, applying digestate fertilizer from biogas production and diluting the topsoil with subsoil. To this end, we hypothesized that (i) erosion induced topsoil dilution and reduction of the C and N contents reduce CO_2 and N_2O emissions from digestate application and that (ii) the soil properties dominated by the erosion state of a soil modify this effect.

2 Materials and Methods

2.1 Studied Soil Types

The investigations were carried out on substrates of a non-eroded Albic Luvisol (Cutanic; LL), eroded Albic Luvisol (Cutanic; eLL), and strongly eroded Calcaric Regosol (RZ) from the erosion-affected "CarboZALF-D" experimental area in the Uckermark region, where tillage erosion is the dominant erosion process. These soils were chosen because they are characteristic of large areas in the northern hemisphere, particularly post-glacial regions (Gerke and Hierold 2012; Rieckh et al. 2012). The Uckermark region is located in the hummocky arable young moraine landscape of northeast Germany (53◦ 23′ N, 13◦ 47′ E; ~50–60 m a.s.l). The site experiences a long-term average annual air temperature

of 9.1 °C and precipitation of 505 mm as recorded by ZALF research station in Dedelow, between the years 2005 to 2020.

The soils in this area are derived from a variety of sandy to marly glacial and glaciofluvial deposits, shaped significantly by soil erosion processes. Consequently, they exhibit distinct soil profiles that reflect different erosion states (Sommer et al. 2008, 2016; Vaidya et al. 2023). In this hummocky moraine landscape, the soil types also represent these erosion states, which are defined by the depth to the parent material (dense glacial till; C horizon; Wilken et al. 2020). The non-eroded Albic Luvisol (LL) retains a clay-eluviated E horizon beneath the Ap, and admixing this E material into the Ap mainly causes SOC dilution but does not substantially alter texture or depth to the C horizon. In the eroded Albic Luvisol (eLL), the E horizon has been removed and the Bt horizon directly underlies the Ap; admixing this Bt material likewise affects SOC but only marginally other soil properties. The strongly eroded Calcaric Regosol (RZ) represents the most advanced erosion stage, where plowing already reaches into the calcareous glacial till, and admixture introduces calcium carbonate ($CaCO_3$)-rich material into the Ap. Thus, the selected soils correspond to realistic erosion states and distinct subsoil horizons that would be mixed into the topsoil under agricultural tillage. Table S1 illustrates notable differences in soil depth, pH values, and texture between the topsoil and subsoil horizons, which are a result of the impact of erosional processes on the development of the soil profile.

2.2 Incubation Experiment Setup and Treatment Preparation

For each soil type, four treatments were prepared: (1) undiluted and unfertilized topsoil (Ap), serving as a control, (2) diluted and unfertilized Ap with 20% material from the respective subsoil horizon (+), (3) undiluted, digestate fertilized Ap material (ORG), and (4) diluted, digestate fertilized Ap with 20% material from the respective subsoil horizon (+ORG). The chosen 20% subsoil admixture reflects the proportion typically incorporated into topsoils during fractional deep tillage or field manipulation experiments in the "CarboZALF-D" experimental area (Deumlich et al. 2017; Sommer et al. 2016; Vaidya et al. 2024; Zentgraf et al. 2024). These treatment abbreviations are used consistently throughout the manuscript. Preparation was conducted as follows: bulk samples from Ap and subsoil horizons from non-eroded Albic Luvisol (LL), eroded Albic Luvisol (eLL), and strongly eroded Calcaric Regosol (RZ) were collected. The samples were air dried and sieved with a 2 mm mesh.

The target aims for preparation were 55% water-filled pore space (WFPS) and a bulk density of 1.4 g cm^{-3}, consistent across all treatments. For the control (undiluted, unfertilized) soils (LL, eLL, RZ), the moisture content of the Ap material was determined, and wet masses were calculated to obtain 4550 g of dry soil. Water (864.4 mL) was added, and the mixture was thoroughly mixed. A total of 415 g of wet soil was placed into each 250 cm^3 piercing cylinder (13 cylinders total) and compacted to the target bulk density. For the +treatment (diluted, unfertilized), the moisture content of both Ap and the respective subsoil horizons was determined. Wet masses were calculated to obtain 3540 g dry Ap and 910 g subsoil material. The appropriate amount of water (864.4 mL) was added, and the soil was thoroughly mixed before being placed into the piercing cylinders and compacted to the target bulk density.

The ORG treatment (undiluted, digestate fertilized) received biogas digestate from the Möllhoff farm (Uckermark): 170 kg NH_4^+-N per ha, i.e. 20 mg NH_4^+-N per 100 g of dry soil. The characteristics of the applied digestate are shown in Table S2. For this treatment, 4550 g of dry Ap material was mixed with 309.4 mL of digestate and the calculated amount of water (excluding the digestate volume) to reach the target water volume of 864.4 mL. The mixture was then transferred into a 250 cm^3 piercing cylinder (13 cylinders in total) and compacted lightly. For +ORG treatment (diluted, digestate fertilized), 3540 g of dry Ap and 910 g of subsoil material were mixed with 309.4 mL of digestate and the appropriate amount of water (excluding the digestate volume) to reach 864.4 mL. The mixture was then transferred into a 250 cm^3 piercing cylinder (13 cylinders in total) and compacted lightly. Additional cylinders were used to assess changes in the soil chemical properties, with 100 cm^3 of wet soil (with or without the admixture and fertilizer, depending on the treatment) repacked into each cylinder at the target bulk density.

2.3 Incubation System and Calculations

To determine the CO_2 and N_2O emissions, the soil samples were transferred to an incubation system presented in detail in Rillig et al. (2021) (Figure S1). According to Livingston and Hutchinson (1995), the system can be described as a flow-through steady-state system, comprised of 16 sealed, cylindrical incubation vessels, each constructed from commercially available KG DN sewer pipes and accessories (Marley, Germany), with a diameter and height of 13 cm. The incubation was conducted under controlled conditions to promote microbial activity and potential N_2O formation. A constant temperature of 20 °C was maintained within the incubation vessels in a controlled climate box, and moisture was adjusted to an optimal 55% WFPS to ensure favorable

conditions for nitrification and denitrification processes (Bateman and Baggs 2005; Chen et al. 2008; Dobbie and Smith 2003). Ambient air, flowing at a rate of 32 mL min^{-1} (determined by flow controller; MKS Instruments GE50A, Andover, MA, USA), was continuously circulated through the headspace of the incubation vessels. A multiplexer was used to connect the different vessels each for 7 min after each other to a cavity ring-down spectroscopy (CRDS) Picarro G2508 gas concentration analyser (PICARRO, INC., Santa Clara, USA). Ambient air circulating directly from the pressure vessel to the gas analyser at the same flow rate, measured once after the 16 vessels served as a reference. Air circulation between the incubation unit headspace and the CRDS analyser was maintained at 250 mL min^{-1} using a low-leak diaphragm pump (A0702, Picarro, Santa Clara, CA, USA). To prevent desiccation of the soil cores, incoming air was pre-saturated to 100% relative humidity before entering the incubation vessels using water traps. The soils were incubated under these conditions for 26 days, during which CO_2 and N_2O emissions were measured.

N_2O and CO_2 fluxes were calculated as follows;

$$F = \frac{(M * \rho * V * (\Delta c))}{(C * R * t * T)} \quad (1)$$

Where F is the flux rate (µg CO_2-C or N_2O-N $core^{-1}$ h^{-1}), M is the molar mass of CO_2 or N_2O, respectively (µg mol^{-1}), ρ the atmospheric pressure (Pa), V is the air flow rate into the headspace and the channels (m^3 h^{-1}), Δc is the difference of gas concentrations [mol] between outlet of a specific vessel and the control channel, C is the core, R the gas constant (m^3 Pa K^{-1} mol^{-1}), t is the time over which the concentration change was observed, and T the incubation temperature (K). Per-core fluxes (F_{core}; µg CO_2-C or N_2O-N $core^{-1}$ h^{-1}) were converted to areal fluxes (F_{area}; µg m^{-2} h^{-1}) by dividing F_{core} by the soil surface area of each incubation core (A_{core}; m^2). Core area (A_{core}) was calculated as $A_{core} = \pi(d/2)^2$, where d is the internal diameter. Because A_{core} is in cm^2, it was converted to m^2 by multiplying by 10^{-4}. An adapted version of an R script developed by Rillig et al. (2021) was used to calculate the current gas flux rates and CO_2-C and N_2O-N gas losses accumulated over time intervals. Additionally, the percentage of fertilizer induced CO_2-C and N_2O-N losses were calculated by subtracting the cumulative CO_2 and N_2O emissions of unfertilized treatments from the cumulative CO_2 and N_2O emissions of fertilized treatments. Thereafter, the percentage (%) of fertilizer induced CO_2-C and N_2O-N losses were calculated by multiplying the CO_2-C and N_2O-N losses by 100 and dividing by the amount of C (973.6 mg) and N (70 mg) that was present in the applied digestate fertilizer (Table 2). Thus, we were able to calculate the fertilizer induced CO_2-C and N_2O-N emissions as fractions of added C and N through fertilization.

2.4 Soil Analyses

Soil samples were collected from the additional 100 cm^3 cylinders at selected times during the 26-day incubation period: t0 (start of the experiment), t1 and t2 (during N_2O peak) and t3 (end of the experiment).

At the time points: t0, t1, t2 and t3 the following soil properties were analysed by the central laboratory at ZALF: ammonium-N (NH_4^+-N), nitrate-N (NO_3^--N), pH value, cold water soluble C (CWSC) and cold water soluble N (CWSN). The determination of NH_4^+-N and NO_3^--N was done according to ISO 14,256 using a CFA-SAN (Skalar analytic GmbH, Breda, Netherlands). The pH values were determined based on ISO 10,390, using a 855 Robotic Titrosampler (Deutsche Metrohm GmbH & Co. KG, Germany) in a 1:5 (volume fraction) suspension of soil in 0,01 mol/L calcium chloride solution (pH in $CaCl_2$). CWSC and CWSN values that reflect the labile C and N pools in the soil were determined with a TOC-V CPH analyser (Shimadzu Deutschland GmbH, Germany). At the end of the experiment (t3), the total C (TC) and total organic carbon (TOC) were analyzed according to ISO 10,694 using a multiphase determinator (RC 612, Leco Instruments GmbH, Mönchengladbach, Germany). Additionally, total N (TN) was analysed at by a CNS928-MLC elemental analyser (LECO Ltd., Germany) according to ISO 13,878. Pedogenic iron (Fe) and aluminum (Al) oxides were characterized by sodium dithionite extraction (Fe_{dith}, Al_{dith}) and acid ammonium oxalate extraction (Fe_{ox}, Al_{ox}) following Schlichting et al. (1995). The Fe and Al concentrations in the extracts were determined by ICP-OES (ThermoFisher SCIENTIFIC GmbH, Germany).

2.5 Statistics

To evaluate the effects of soil type (erosion state), topsoil dilution, and digestate fertilisation, we performed a three-way analyses of variance (ANOVA) on cumulative CO_2-C and N_2O-N emissions, fertilizer-induced C and N losses, and final soil chemical properties (TC, TOC, TN, Al_{ox}, Al_{dith}, Fe_{ox}, and Fe_{dith}). These models considered the three factors as fixed effects and their interactions. Where ANOVA assumptions were met, post hoc pairwise comparisons were conducted using Tukey's Honest Significant Difference (HSD) test ($\alpha = 0.05$). The normality of residuals was evaluated using the Kolmogorov-Smirnov test, and homogeneity of variances was assessed using Levene's test. Residual plots were also visually inspected. In cases where normality assumptions were violated and could not

be corrected by transformation (e.g., for cumulative N_2O emissions) non-parametric Kruskal Wallis tests were used, followed by Dunn's test for pairwise comparisons with Bonferroni correction.

For CWSC (Table S4) CWSN (Table S5), NH_4^+-N (Table S6), and NO_3^--N concentrations (Table S7), linear mixed-effects models (LMMs) were used to assess the effects of fertilization, topsoil dilution, soil type, time, and their interactions. Time point (t0–t3) was modelled as a fixed effect, while replicate ID was included as a random effect to account for repeated measures. Post hoc pairwise comparisons were conducted on estimated marginal means (EMMs) using Tukey adjustment for multiple testing.

Dynamic CO_2 (Table S8) and N_2O fluxes (Table S9) over time were analysed separately using LMMs, with fixed effects for treatment, day of measurement (DOM), and their interaction (Treatment x DOM), and random intercepts for experimental repetitions. Separate models were fitted for different treatment groups (e.g., undiluted soils, diluted soils, fertilized soils, and their combinations). EMMs and pairwise Tukey-adjusted contrasts were extracted to identify significant differences between treatments over time.

All data are presented as means ± standard deviation (SD). Compact letter displays were used to denote significant differences between treatments. All statistical analyses were conducted in R version 4.2.1 (R Core Team, 2022).

3 Results

3.1 Erosion-Induced Topsoil Dilution Effects on Stable and Dynamic Soil Properties

TC (%) decreased in the LL and eLL soils as a result of topsoil dilution, regardless of fertilizer addition. However, in the RZ soil, topsoil dilution did not significantly affect the unfertilized treatment, while there was a slight increase in the fertilized treatment compared to the other soil types. In addition, the consistently clear difference between TC (%) and TOC (%) contents in the RZ indicates a significantly higher proportion of carbonate C than in the other soils. TOC (%) decreased across all soil types, in both the fertilized and unfertilized treatments. TN (%) decreased slightly as a result of topsoil dilution only in the fertilized treatment of the LL soil, while both fertilized and unfertilized treatments of the eLL and RZ soils showed a slight decrease (Table 1). Additionally, topsoil dilution slightly increased the clay bound Al and Fe oxide (Al_{ox}, Al_{dith}, Fe_{ox}, Fe_{dith}) contents (mg kg^{-1}) in the eLL soil, while only minor changes were observed in LL and RZ. Fertilization caused small increases in Al_{ox} in LL and eLL and in Fe_{ox} contents in eLL, whereas the other oxide forms remained largely unchanged. In the fertilized treatments, topsoil dilution led to a slight increase in oxide contents in eLL, but small decreases or no clear changes in LL and RZ (Table S3).

Table 1 Soil chemical properties ((%) soil dry matter (DM)), including total soil carbon (TC), total soil organic carbon (TOC) and total soil nitrogen (TN) for different soil types and erosion states: non-eroded albic luvisol (LL), eroded albic luvisol (eLL), and strongly eroded calcaric regosol (RZ), at the end of the experiment (t3), after 26 days. Treatments include control (undiluted, unfertilized), + (diluted, unfertilized), ORG (undiluted, digestate fertilized), and +ORG (diluted, digestate fertilized). The displayed values represent the mean of the replicate treatments ± standard deviation ($n=4$). Letters represent statistically significant variations (p-value, 0.05 threshold) among the treatments, based on the three-way ANOVA

Soil type	TC (% soil DM)	TOC (% soil DM)	TN (% soil DM)
LL	$0.61^{h} \pm 0.01$	$0.59^{e} \pm 0.01$	$0.06^{e} \pm 0.01$
+LL	$0.54^{i} \pm 0.02$	$0.52^{f} \pm 0.02$	$0.05^{e} \pm 0.01$
LL ORG	$0.84^{ef} \pm 0.04$	$0.82^{c} \pm 0.04$	$0.10^{ab} \pm 0.01$
+LL ORG	$0.73^{g} \pm 0.02$	$0.71^{d} \pm 0.02$	$0.09^{bc} \pm 0.00$
eLL	$0.79^{fg} \pm 0.03$	$0.73^{d} \pm 0.03$	$0.08^{cd} \pm 0.01$
+eLL	$0.66^{h} \pm 0.02$	$0.61^{e} \pm 0.02$	$0.06^{de} \pm 0.00$
eLL ORG	$1.01^{d} \pm 0.01$	$0.95^{a} \pm 0.01$	$0.11^{ab} \pm 0.01$
+eLL ORG	$0.88^{e} \pm 0.01$	$0.83^{bc} \pm 0.00$	$0.10^{a} \pm 0.01$
RZ	$1.11^{c} \pm 0.02$	$0.72^{d} \pm 0.02$	$0.08^{c} \pm 0.00$
+RZ	$1.15^{c} \pm 0.04$	$0.56^{ef} \pm 0.04$	$0.07^{de} \pm 0.00$
RZ ORG	$1.26^{b} \pm 0.02$	$0.89^{b} \pm 0.01$	$0.11^{a} \pm 0.01$
+RZ ORG	$1.37^{a} \pm 0.05$	$0.79^{c} \pm 0.02$	$0.10^{ab} \pm 0.01$

CWSC concentrations (mg kg^{-1} soil) were consistently higher in digestate-fertilized soils across all time points. Topsoil dilution had no significant effect within soil types, except at t1, where CWSC was lower in +eLL ORG compared to eLL ORG. CWSC increased over time in fertilized soils, while unfertilized treatments showed low CWSC throughout the experiment. No differences were found between diluted and undiluted soils in unfertilized treatments (Fig. 1a–c).

CWSN concentrations (mg kg^{-1} soil) were consistently higher in digestate-fertilized soils across all time points. Topsoil dilution generally had no significant effect within soil types, although in a few cases (e.g., +eLL ORG at t0, +LL ORG and +RZ ORG at t1 and t3), diluted treatments showed slightly lower CWSN than their undiluted counterparts. CWSN increased over time in fertilized soils, particularly between t2 and t3, while remaining low in unfertilized soils (Fig. 1d–f).

NH_4^+-N concentrations (mg kg^{-1} soil)were consistently higher in digestate-fertilized soils across all soil types, especially at early time points. Topsoil dilution generally had no significant effect on NH_4^+-N concentrations within fertilized soils. However, at t1, NH_4^+-N was significantly lower in the diluted eLL ORG treatment compared to eLL ORG, indicating a short-term dilution effect. NH_4^+-N

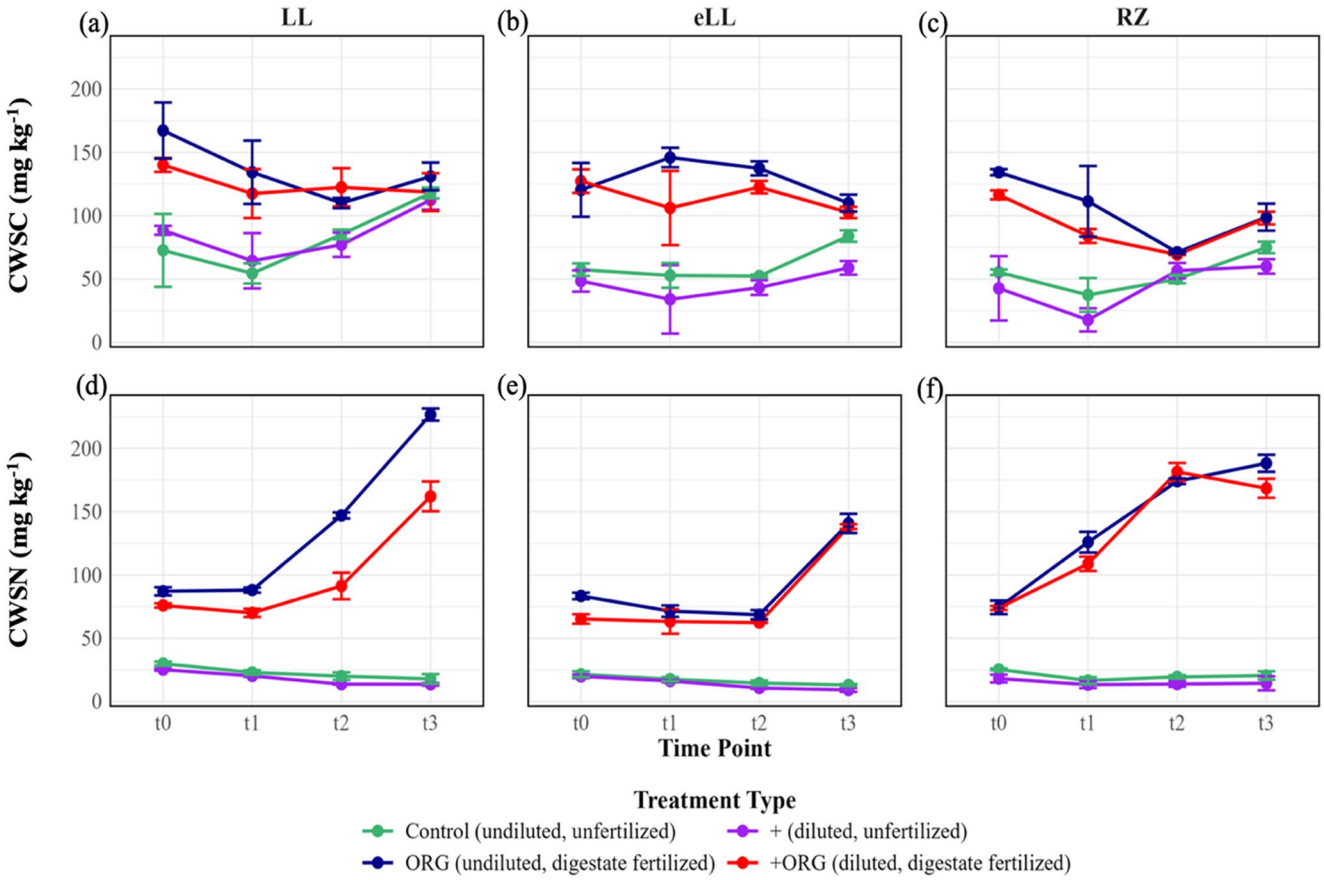

Fig. 1 Dynamics of cold water soluble carbon (CWSC; top row) and nitrogen (CWSN; bottom row) concentrations (mg kg^{-1} soil) across four time points (t0, t1, t2, t3) for different soil types and erosion states: (**a**, **d**) non-eroded Albic Luvisol (LL), (**b**, **e**) eroded Albic Luvisol (eLL), and (**c**, **f**) strongly eroded Calcaric Regosol (RZ). Treatments include control (undiluted, unfertilized; green), + (diluted, unfertilized; purple), ORG (undiluted, digestate fertilized; blue), and +ORG (diluted, digestate fertilized; red). Statistical analysis was conducted using linear mixed-effects models (LMMs), with replicate ID as a random effect to account for repeated measurements across time. Fixed effects included fertilization, topsoil dilution, soil type, time, and their interactions. Data represent means of independent replicates ($n = 3$ for t0–t2; $n = 4$ for t3). Error bars indicate ± 1 standard deviation

levels declined rapidly over time in all fertilized treatments, approaching zero by the end of the incubation. In unfertilized soils, NH_4^+-N remained low throughout the experiment (Fig. 2a–c).

NO_3^--N concentrations (mg kg^{-1} soil) increased substantially over time in digestate-fertilized soils, reaching peak levels at t3. Topsoil dilution had no consistent effect overall, though at t1, the undiluted LL ORG treatment had significantly higher NO_3^--N than the diluted LL treatment. In unfertilized treatments, NO_3^--N levels remained low and showed only minor variation throughout the incubation. These trends align with significant treatment-by-time interactions detected in the statistical analysis (Fig. 2d–f).

3.2 CO_2 and N_2O Flux Dynamics

CO_2 fluxes (µmol m^{-2} s^{-1}) varied significantly across different soil types and erosion states, with the highest fluxes observed in the LL soil, followed by eLL, and the lowest in the RZ soil (Fig. 3a). Topsoil dilution significantly reduced CO_2 fluxes in the LL and RZ compared to their undiluted counterparts, with the greatest reduction observed in the LL, followed by RZ, and a slight increase observed in the eLL (Fig. 3b). Digestate application led to a significant increase in CO_2 fluxes across all soils, with the strongest effect observed in the RZ, followed by LL, and a moderate increase in the eLL (Fig. 3c). In fertilized soils (LL ORG, eLL ORG, RZ ORG), topsoil dilution significantly reduced CO_2 fluxes, with the most pronounced reduction in the LL ORG, followed by eLL ORG, and a smaller reduction observed in the RZ ORG treatment (Fig. 3d).

N_2O fluxes (µmol m^{-2} s^{-1}) varied by soil type, with the highest emissions observed in the RZ soils, followed by LL and eLL soils (Fig. 4a). Topsoil dilution significantly reduced N_2O fluxes in all soil types compared to their undiluted (LL, eLL and RZ) counterparts (Fig. 4b). Digestate addition significantly increased N_2O emissions across all soil types, with the eLL ORG showing significantly higher

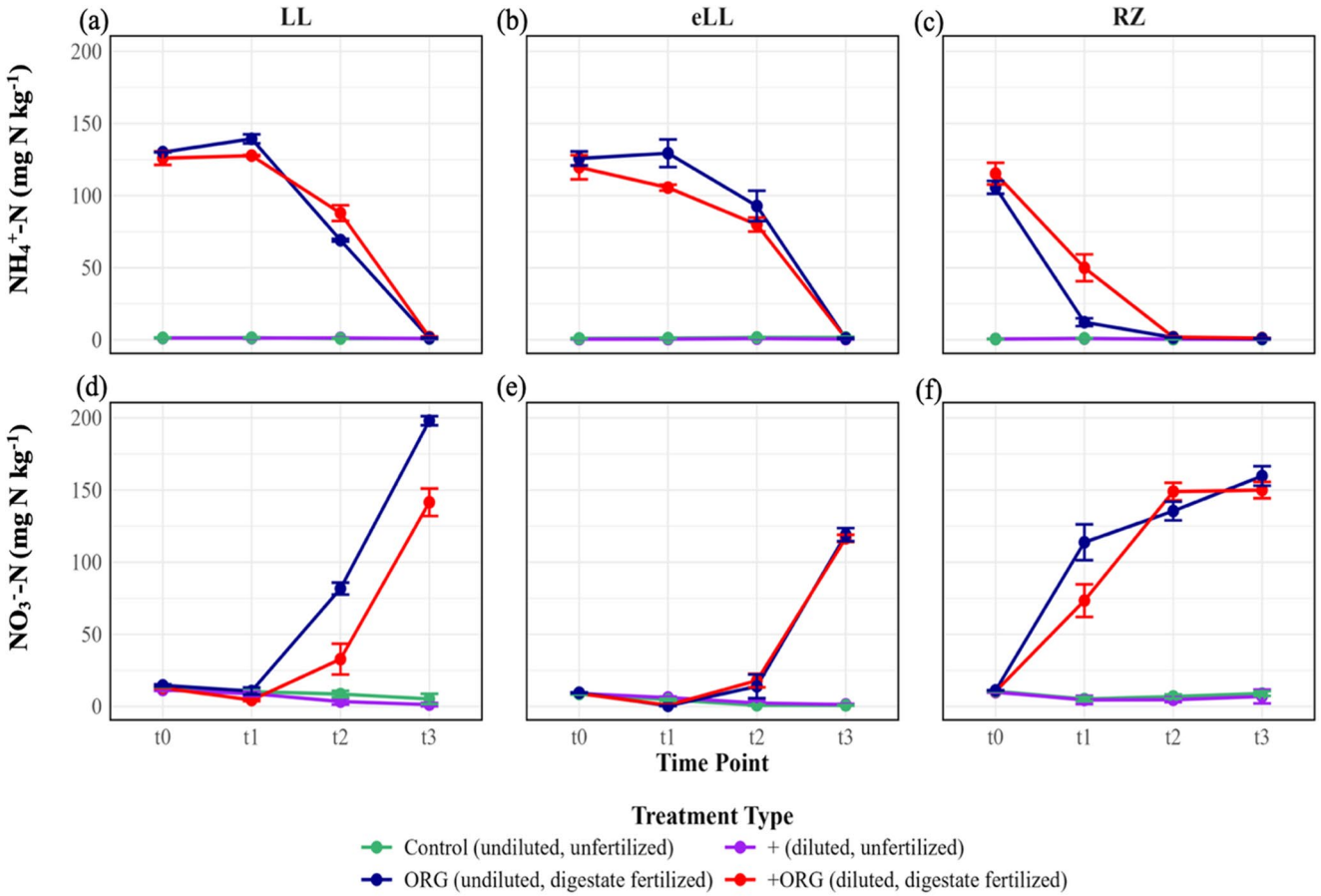

Fig. 2 Dynamics of ammonium (NH_4^+-N; top row) and nitrate (NO_3^--N; bottom row) concentrations (mg N kg^{-1} soil) across four time points (t0, t1, t2, t3) for different soil types and erosion states: (**a**, **d**) non-eroded Albic Luvisol (LL), (**b**, **e**) eroded Albic Luvisol (eLL), and (**c**, **f**) strongly eroded Calcaric Regosol (RZ). Treatments include control (undiluted, unfertilized; green), + (diluted, unfertilized; purple), ORG (undiluted, digestate fertilized; blue), and +ORG (diluted, digestate fertilized; red). Statistical analysis was conducted using linear mixed-effects models (LMMs), with replicate ID as a random effect to account for repeated measurements across time. Fixed effects included fertilization, topsoil dilution, soil type, time, and their interactions. Data represent means of independent replicates ($n = 3$ for t0–t2; $n = 4$ for t3). Error bars indicate ± 1 standard deviation

emissions than the LL ORG and RZ ORG (Fig. 4c) Topsoil dilution significantly increased N_2O fluxes in the +LL ORG and +RZ ORG compared to their undiluted fertilised counterparts (LL ORG and RZ ORG), whereas in +eLL ORG, fluxes were significantly lower than in eLL ORG (Fig. 4d).

3.3 Cumulative C and N Losses by CO_2 and N_2O

The cumulative CO_2 emission (mg CO_2-C $core^{-1}$) of the LL soil was the highest compared to eLL and RZ soils which had similar values among each other (Table 2). Topsoil dilution resulted in a decrease in the cumulative CO_2 emissions in the +LL soil, while no differences were observed in the +eLL and +RZ soils. Digestate addition increased cumulative CO_2 emissions in all soil types, while topsoil dilution decreased cumulative CO_2 emissions in all these fertilized soil types. Unfertilized treatments showed the lowest N_2O emissions (mg N_2O-N $core^{-1}$) and there were no statistically significant differences between soils with and without topsoil dilution. The eLL ORG soil had the highest N_2O emissions, followed by RZ ORG and LL ORG. Topsoil dilution increased cumulative N_2O emissions in the +LL ORG and +RZ ORG, particularly in the +RZ ORG treatment. In contrast, topsoil dilution decreased N_2O emissions in the +eLL ORG treatment. Fertilizer-induced CO_2-C losses (%) were similar in the eLL ORG and RZ ORG, while LL ORG had the lowest amount. Fertilizer-induced CO_2-C losses decreased significantly with topsoil dilution in the +LL ORG and +eLL ORG soils. This trend was only slightly visible for the +RZ ORG. The eLL ORG had the highest amount of fertilizer induced N_2O-N losses (%). The LL ORG and RZ ORG treatments showed similar values, both lower than the amount of fertilizer-induced N_2O-N losses of the eLL ORG. Fertilizer N_2O-N losses were not significantly affected by topsoil dilution in the +LL ORG. However, there was a significant increase in the +RZ ORG

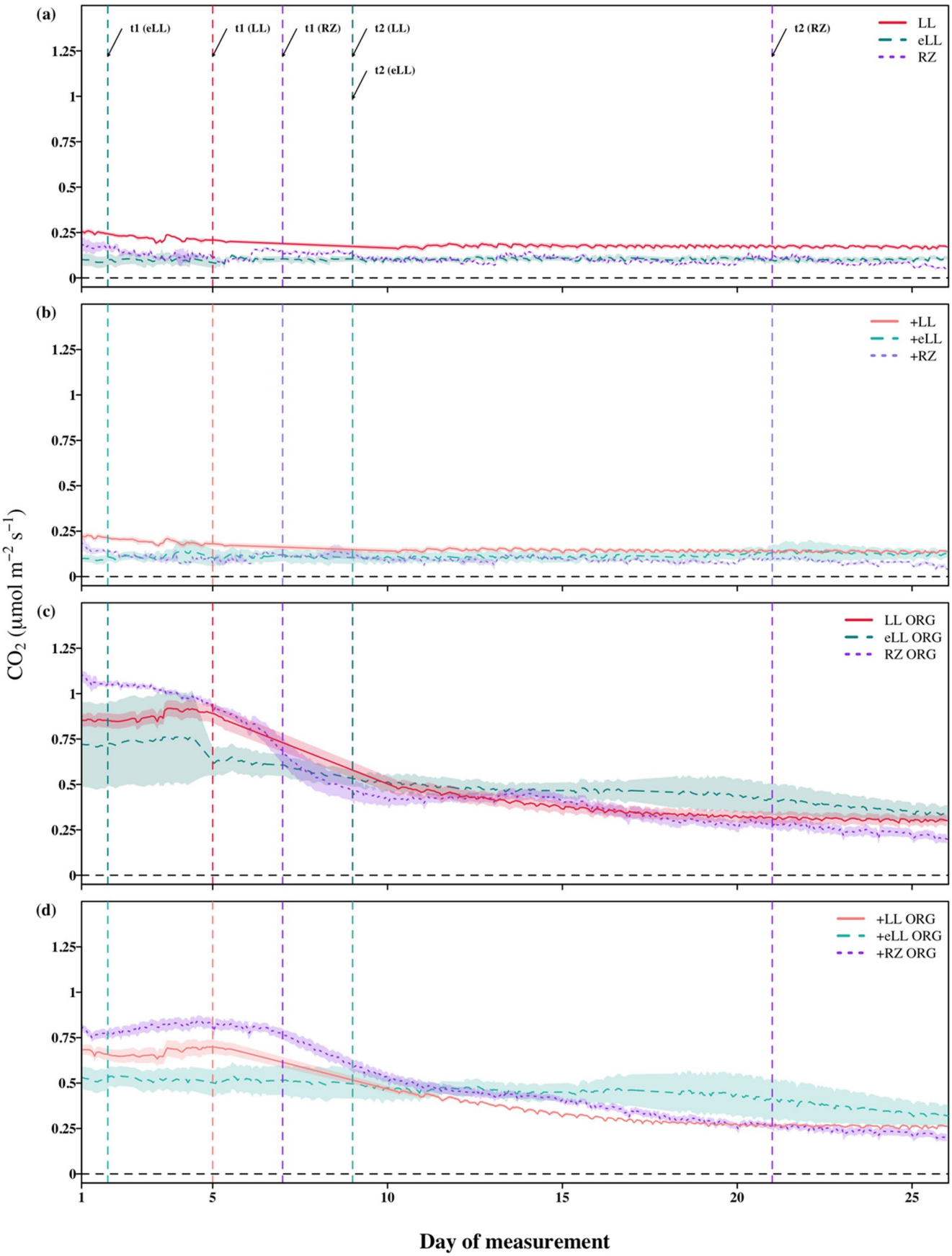
(a)
t1 (eLL)
t1 (LL)
t1 (RZ)
t2 (LL)
t2 (eLL)
t2 (RZ)
LL
eLL
RZ
(b)
+LL
+eLL
+RZ
(c)
LL ORG
eLL ORG
RZ ORG
(d)
+LL ORG
+eLL ORG
+RZ ORG
CO2 (µmol m−2 s−1)
Day of measurement

Fig. 3 CO_2 flux dynamics (µmol m^{-2} s^{-1}) over the 26-day measurement period. Lines represent soil types and erosion states: non-eroded Albic Luvisol (LL; red, solid), eroded Albic Luvisol (eLL; turquoise, dashed), and strongly eroded Calcaric Regosol (RZ; purple, dotted). Panels show different treatments: (**a**) control (undiluted, unfertilized), (**b**) + (diluted, unfertilized), (**c**) ORG (undiluted, digestate fertilized), and (**d**) + ORG (diluted, digestate fertilized). Shaded areas represent ± 1 standard deviation (SD). Vertical dashed lines show soil sampling at t1 and t2 (during the N_2O peak); colors match the respective soil types/treatments. LL and eLL overlap at t2. t0 (start) and t3 (end) coincide with the measurement period limits and are omitted for clarity. Fluxes were analyzed using separate linear mixed-effects models (LMMs) fitted for each soil group, with fixed effects for treatment (soil type, dilution, fertilization), day of measurement (DOM), and their interaction, and random intercepts for experimental repetitions. Pairwise differences between treatments were assessed using estimated marginal means (EMMs) with Tukey adjustment

and a significant decrease in + eLL ORG due to topsoil dilution (Table 2).

4 Discussion

This study investigated how erosion-induced topsoil dilution influences CO_2 and N_2O emissions following digestate application, testing two hypotheses: (i) erosion induced topsoil dilution and reduction of the C and N contents reduce CO_2 and N_2O emissions from digestate application and that (ii) the soil properties dominated by the erosion state of a soil modify this effect. The results confirmed that digestate application consistently increased CO_2, and more strongly N_2O emissions across all soils. However, topsoil dilution mitigated CO_2 emissions in all digestate-fertilized soils, with a significant reduction observed only in the non-eroded (LL) soil. This indicates that while the direction of the dilution effect was uniform, its strength depended on erosion severity, thereby supporting both hypotheses for CO_2 emissions. In contrast, N_2O responses were more variable: dilution reduced emissions in the moderately eroded (eLL) soil but increased them in the strongly eroded (RZ) soil, and slightly in LL. Consequently, the first hypothesis was only partially supported for N_2O, whereas the second hypothesis was clearly confirmed. These findings suggest that management strategies on eroded soils should consider the erosion state when applying digestate, as the same input may have contrasting effects on CO_2 and N_2O emissions.

Digestate addition significantly increased CO_2 emissions across all soil types, as reflected in both flux measurements and cumulative emissions (Table 2; Fig. 3c). This increase corresponds with higher TOC levels (Table 1) as well as higher CWSC (Fig. 1a-c) following digestate application, suggesting that the added organic material provided readily available C sources that enhanced soil respiration and CO_2 release. These findings align with previous studies reporting elevated CO_2 emissions after digestate application due to increased substrate availability for decomposition (Alburquerque et al. 2012; Bol et al. 2003; Fangueiro et al. 2010; Pezzolla et al. 2012; Rochette et al. 2000). Topsoil dilution, however, reduced CO_2 fluxes in digestate-fertilized soils across all erosion stages (Fig. 3d), but cumulative CO_2 emissions showed a statistically significant reduction only in the non-eroded LL soil (Table 2). This indicates that while the direction of the dilution effect was consistent, its magnitude varied, with the most pronounced mitigation occurring in LL. A similar trend was observed in unfertilized soils: fluxes decreased slightly with dilution in LL and RZ but remained unchanged or increased in eLL (Fig. 3b), again with only LL showing a significant overall reduction (Table 2). These findings suggest that the capacity of topsoil dilution to reduce CO_2 emissions is strongest in non-eroded soils, likely due to the decline in TOC following the incorporation of C-poor subsoil (Table 1). The decrease in SOC aligns with previous studies showing that topsoil removal reduces C and nutrient availability and alters microbial community composition (Allison and Ausden 2004; Geissen et al. 2013; Niemeyer et al. 2007; Pehlivan et al. 2025; Ruggaber et al. 2024; Zentgraf et al. 2024). However, our results indicate that the effect of topsoil dilution differs based on digestate application. Specifically, in the first 13 days of the experiment, the difference in CO_2 emissions between digestate-applied (Fig. 3d) and non-applied treatments (Fig. 3b) was substantial. In the remaining days, the emissions became more similar, although some differences persisted, likely due to enhanced microbial activity stimulated by digestate addition (Fig. 3d and b). Overall, this pattern suggests that topsoil dilution not only reduces SOC and CO_2 emissions but may also facilitate the retention of C from digestate in the soil.

One potential mechanism underlying this C retention could be the enhanced stabilization of digestate-derived OC through sorptive interactions with subsoil clay minerals. Less saturated subsoil clay minerals offer more binding sites, allowing digestate-derived C to associate with mineral surfaces, thereby reducing its bioavailability (Baldock and Skjemstad 2000; Hassink and Whitmore 1997; Kaiser and Guggenberger 2003; Kögel-Knabner et al. 2008; Sollins et al. 2009; Spielvogel et al. 2008). As mentioned, this dilution of SOC stocks likely resulted in a C undersaturation, increasing the soil's capacity for additional C input (Berhe and Kleber 2013; Doetterl et al. 2016; Hassink, 1997; Stewart et al. 2007; Xiao et al. 2018). Within this context, the concept of "dynamic replacement" might help explain the observed trend. Topsoil dilution promotes the temporary accumulation of fresh OC, in this case, OC from digestate, within the diminished C stock due to topsoil dilution, thereby reducing CO_2 fluxes (Dialynas et al. 2017; Doetterl et al. 2016; Harden et al. 1999; Hoffmann et al. 2017,

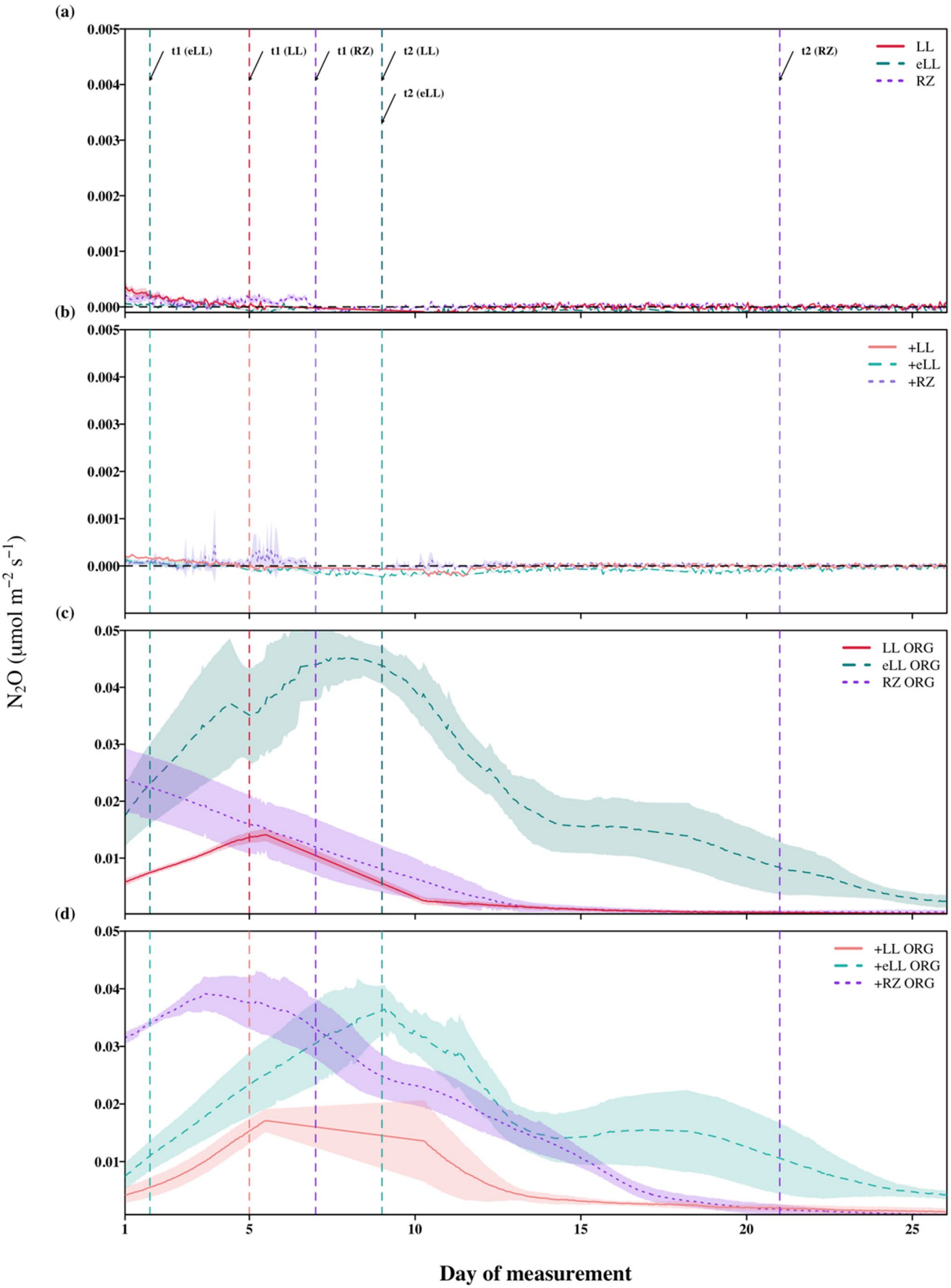
(a)
(b)
(c)
(d)
t1 (eLL)
t1 (LL)
t1 (RZ)
t2 (LL)
t2 (eLL)
t2 (RZ)
LL
eLL
RZ
+LL
+eLL
+RZ
LL ORG
eLL ORG
RZ ORG
+LL ORG
+eLL ORG
+RZ ORG
N2O (µmol m−2 s−1)
Day of measurement

Fig. 4 N_2O flux dynamics (µmol m^{-2} s^{-1}) over the 26-day measurement period. Lines represent soil types and erosion states: non-eroded Albic Luvisol (LL; red, solid), eroded Albic Luvisol (eLL; turquoise, dashed), and strongly eroded Calcaric Regosol (RZ; purple, dotted). Panels show different treatments: (**a**) control (undiluted, unfertilized), (**b**) + (diluted, unfertilized), (**c**) ORG (undiluted, digestate fertilized), and (**d**) + ORG (diluted, digestate fertilized). Shaded areas represent ± 1 standard deviation (SD). Vertical dashed lines show soil sampling at t1 and t2 (during the N_2O peak); colors match the respective soil types/treatments. LL and eLL overlap at t2. t0 (start) and t3 (end) coincide with the measurement period limits and are omitted for clarity. Fluxes were analysed using separate linear mixed-effects models (LMMs) fitted for each soil group, with fixed effects for treatment (soil type, dilution, fertilization), day of measurement (DOM), and their interaction, and random intercepts for experimental repetitions. Pairwise differences between treatments were assessed using estimated marginal means (EMMs) with Tukey adjustment

2018; Lal 2019), possibly leading to enhanced C sequestration. However, given the short duration of the experiment, it remains unclear whether this change in SOC represents true stabilization or merely a temporary accumulation of labile OC. Future studies should test whether such C stabilization persists under field conditions and over longer timescales to capture long-term SOC dynamics.

The erosion state further influenced the pattern of topsoil dilution effects on CO_2 emissions, particularly in the flux dynamics. The reduction in emissions with dilution appeared to diminish with increasing erosion severity, as seen in the flux data (Fig. 3d), possibly because highly eroded soils are already C-undersaturated, limiting the potential of dilution to further reduce emissions (Hassink, 1997; Holz and Augustin 2021; Stewart et al. 2009; West and Six 2007). Notably, the effect of dilution was more pronounced in digestate-fertilized soils, where the added organic material likely enhanced C retention and temporarily mitigated CO_2 emissions across all erosion stages (Levavasseur et al. 2022; Reuland et al. 2022). Nevertheless, cumulative CO_2 emissions (Table 2) showed a statistically significant reduction only in the non-eroded LL soil, indicating that while the direction of the dilution effect was consistent, its magnitude and duration varied with erosion severity. This pattern suggests that the potential for C retention through dilution is highest in non-eroded soils, while in more eroded soils, the existing C-undersaturation (Table 1) may limit this response over time. Overall, these findings confirm that erosion severity modulates the capacity of soils to retain C inputs from digestate and that the mitigation effect of topsoil dilution on CO_2 emissions is most effective under non-eroded conditions.

Beyond CO_2 dynamics, digestate application also had a pronounced influence on N_2O emissions, although the response to topsoil dilution was more variable among soils. Digestate addition significantly increased N_2O emissions across all soil types (Fig. 4c; Table 2), consistent with the observed rise in TN levels (Table 1) and CWSN concentrations (Fig. 1d-f), indicating greater availability of mineralizable N for microbial processes. This was expected given the high NH_4^+-N content of the digestate, which provided a readily available N source for microbial nitrification and denitrification processes (Dietrich et al. 2020; Ma et al. 2011; Wang et al. 2014). Elevated NH_4^+-N concentrations in fertilized soils during the early stages (Fig. 2a-c) and increased NO_3^--N levels at later stages (Fig. 2d-f) promote microbial activity and N transformation processes, causing high N_2O emissions (Batlle-Aguilar et al. 2011; Groffman et al. 2002). While topsoil dilution generally led to reduced CO_2 fluxes, its effect on N_2O emissions was more variable, reflecting the complex and soil-dependent nature of N cycling. Specifically, N_2O emissions were reduced in the moderately eroded eLL soil, increased in the strongly eroded RZ soil and showed a smaller, non-significant increase in the LL soil (Fig. 4d; Table 2). These contrasting responses suggest that the influence of topsoil dilution is not solely governed by erosion status, but also by underlying soil properties. This finding highlights key differences between C and N cycling in agroecosystems, as well as their interactions with digestate properties and soil characteristics (de la Fuente et al. 2013; Möller 2015; Reuland et al. 2022). While CO_2 emissions are largely controlled by TOC levels (Doetterl et al. 2016; Hoffmann et al. 2017, 2018; Lal 2019; Vaidya et al. 2021), N_2O emissions are influenced by a broader set of interacting soil properties such as texture, pH, $CaCO_3$ and reactive mineral oxides, that jointly regulate N cycling (Bingham and Cotrufo 2016; Lützow et al. 2006; Yu et al. 2013). Consequently, the varying effects of dilution on these soil properties influence N transformation processes, leading to an inconsistent response in N_2O emissions across different soils.

The moderately eroded eLL soil showed the most distinct response topsoil dilution, with marked reduction in N_2O emissions attributable to its clay-rich subsoil and enrichment in Fe and Al oxides. Among all soils, the eLL soil contained the highest clay content overall, and its Bt subsoil was particularly clay-rich (≈19%; Table S1). After dilution, the total clay content increased only slightly (from 14% to 15%), reflecting the minor effect of subsoil admixture rather than a statistically significant difference. However, this modest increase was accompanied by a higher abundance of reactive clay-associated minerals, as indicated by the elevated oxalate- and dithionite-extractable Al and Fe concentrations (Table S3). Previous studies on the similar soil type confirm its elevated clay fraction and oxide enrichment (Pehlivan et al. 2025; Remus et al. 2018). X-ray diffraction (XRD) analyses showed illite (30%), illite-smectite mixed-layer minerals (65%), kaolinite (5%), and traces of chlorite (Remus et al. 2018), supporting the high cation-binding capacity of the diluted eLL soil. Consistent with these properties, the

Table 2 Cumulative (26 days) CO_2 (mg CO_2-C $core^{-1}$) and N_2O (mg N_2O-N $core^{-1}$) emissions, fertilizer induced C and N losses as CO_2-C (%) and N_2O-N (%) for different soil types and erosion states: non-eroded albic luvisol (LL), eroded albic luvisol (eLL), and strongly eroded calcaric regosol (RZ). Treatments include control (undiluted, unfertilized), + (diluted, unfertilized), ORG (undiluted, digestate fertilized), and +ORG (diluted, digestate fertilized). Percentage losses of CO_2-C and N_2O-N were calculated relative to the amount of C (973.6 mg) and N (70 mg) applied via digestate fertilizer. Values represent means ± standard deviation ($n = 4$). Statistical analysis was performed using three-way ANOVA with soil type, topsoil dilution, and fertilisation as fixed factors. Where significant effects were detected, tukey's HSD was used for post hoc comparisons. For N_2O, which violated ANOVA assumptions (non-normal residuals, $p < 0.01$), Kruskal-Wallis and dunn's post hoc tests (Bonferroni-corrected) were applied. Different letters indicate statistically significant differences between treatments ($p < 0.05$)

Treatment	CO_2 (mg CO_2-C $core^{-1}$)	N_2O (mg N_2O-N $core^{-1}$)	Fertilizer induced CO_2-C losses (%)	Fertilizer induced N_2O-N losses (%)
LL	$5.73^{d} \pm 0.34$	$0.004^{b} \pm 0.002$	-	-
+LL	$4.81^{de} \pm 0.36$	$-0.001^{b} \pm 0.001$	-	-
LL ORG	$15.66^{ab} \pm 1.15$	$0.26^{a} \pm 0.03$	$1.02^{bc} \pm 0.10$	$0.36^{c} \pm 0.05$
+LL ORG	$13.36^{c} \pm 0.22$	$0.52^{a} \pm 0.06$	$0.88^{c} \pm 0.05$	$0.75^{c} \pm 0.09$
eLL	$3.12^{e} \pm 0.55$	$-0.003^{b} \pm 0.001$	-	-
+eLL	$3.39^{e} \pm 0.76$	$-0.012^{b} \pm 0.006$	-	-
eLL ORG	$15.85^{ab} \pm 1.89$	$1.54^{a} \pm 0.17$	$1.31^{a} \pm 0.19$	$2.20^{a} \pm 0.25$
+eLL ORG	$13.97^{bc} \pm 0.44$	$1.22^{a} \pm 0.10$	$1.09^{abc} \pm 0.11$	$1.76^{b} \pm 0.15$
RZ	$3.34^{e} \pm 0.11$	$0.005^{b} \pm 0.001$	-	-
+RZ	$3.01^{e} \pm 0.25$	$-0.002^{b} \pm 0.002$	-	-
RZ ORG	$16.00^{a} \pm 0.79$	$0.49^{a} \pm 0.17$	$1.30^{a} \pm 0.07$	$0.69^{c} \pm 0.25$
+RZ ORG	$15.22^{abc} \pm 0.54$	$1.21^{a} \pm 0.14$	$1.25^{ab} \pm 0.04$	$1.74^{b} \pm 0.21$

eLL soil exhibited slower mineral N turnover than LL and RZ, showing a more gradual decline in NH_4^+-N and delayed accumulation of NO_3^--N accumulation (Fig. 2), which indicates inherently slower N transformation processes. Such clay-rich subsoil material can store organic compounds and mineral N forms like NH_4^+-N, temporarily protecting them from microbial transformation and plant uptake (Berhe et al. 2018; Castellano et al. 2012; Schoof et al. 2025; Zentgraf et al. 2024). The large surface area and reactive minerals provide sorption sites for NH_4^+-N and organic N, reducing substrate availability for denitrification (Bingham and Cotrufo 2016; Knicker 2011; Lützow et al. 2006; Rillig et al. 2007; van Groenigen et al. 2015;). Consequently, N becomes less available for microbial processes responsible for N_2O production (Vogel et al. 2014, 2015), explaining the observed reduction in N_2O emissions and the lower fertilizer-induced N_2O-N (Table 2). Nevertheless, the specific mechanism of N retention under digestate application and topsoil dilution remains unclear and requires further investigation. Future studies should identify which soil fractions and clay minerals are involved in N stabilization, determine how long the retained N persists, and assess the extent to which these processes contribute to long-term mitigation of N_2O emissions. Combining isotopic tracing with fractionation analyses would further clarify how mineral-organic interactions control N stabilization under digestate amendment.

In contrast to the eLL soil, the strongly eroded RZ soil responded to topsoil dilution with an increase in N_2O emissions (Table 2; Fig. 4d), possibly reflecting the influence of its distinct calcareous properties and relatively higher pH. As shown in Table S1, RZ already had calcareous conditions in the Ap horizon (pH 7.2; $CaCO_3$ 3.2%), and mixing 20% subsoil Cc (pH 7.4; $CaCO_3 \approx 11.6\%$) leaves its pH essentially unchanged (expected ≈ 7.2) while increasing $CaCO_3$ (≈4.9%). Even after dilution, RZ maintained the highest pH compared to LL (≈5.7) and eLL (≈6.7). Together with the increased $CaCO_3$ content, this may promote a higher nitrification potential and thus likely contributed to the enhanced N_2O release observed in this soil (Table S1; Ciu et al. 2012; Gao et al. 2023; Kyveryga et al. 2004; Sahrawat 2008; Tao et al. 2017). Supporting this interpretation, NO_3^--N and NH_4^+-N dynamics revealed rapid NH_4^+-N depletion between t0 and t1 (Fig. 2c and f), coinciding with an early N_2O emission peak, which suggests accelerated N turnover and increased nitrification. In contrast, the LL and eLL soils showed slower NH_4^+-N decline between t2 and t3 (Fig. 2a and b), accompanied by delayed N_2O peaks (Batlle-Aguilar et al. 2011; Groffman et al. 2002). Thus, in RZ, the combination of calcareous conditions and rapid N turnover promoted greater N_2O production under dilution, contrasting with the more subdued response observed in LL soils.

In the LL soil, topsoil dilution led to only subtle changes in N_2O emissions, with no statistically significant increase in cumulative fluxes (Table 2). Nevertheless, fluxes exhibited a slightly prolonged peak (Fig. 4d), corresponding with the observed NH_4^+-N and NO_3^--N dynamics, where NH_4^+-N declined sharply between t1 and t2 and NO_3^--N increased thereafter (Fig. 2a and d). This pattern reflects an intermediate timing of N transformation relative to the faster turnover in RZ and the slower processes in eLL. The diluted

LL treatment (+LL ORG) also showed lower CWSN during the N_2O peak (t1–t2) and again at t3, suggesting enhanced N turnover and reduced retention of mineral N over time (Fig. 1d). This effect likely resulted from mixing C- and N-poor subsoil into the topsoil, which lowered TOC and TN contents (Table 1) and consequently reduced the C: N ratio. Under these conditions, microbial communities may experience an excess of available N relative to C, limiting immobilization and promoting N losses as N_2O (Akiyama et al. 2020; Baggs et al. 2000; Yao et al. 2022). The minor increase in N_2O emissions in LL therefore likely reflects a temporary acceleration of N cycling rather than structural differences in soil properties or inherent N availability.

It is important to note that the soils studied (LL, eLL, and RZ) represent distinct erosion states that also differ in parent material and chemistry, such as the carbonate-rich subsoil in RZ (Sommer et al. 2016; Wilken et al. 2020). These inherent differences likely influenced GHG responses alongside erosion effects. Overall, our results show that erosion-induced topsoil dilution alters CO_2 and N_2O emissions by modifying C and N availability and related microbial processes, underscoring the importance of erosion-aware management when applying organic fertilizers. Integrating such erosion-aware strategies with remote or proximal sensing approaches could support site-specific fertilizer management to improve nutrient efficiency and mitigate GHG emissions.

5 Conclusions

This study demonstrated that erosion-induced topsoil dilution affects carbon dioxide (CO_2) and nitrous oxide (N_2O) emissions following digestate application differently. Using soil types as proxies for erosion introduces inherent differences in parent material, yet this approach reflects realistic field conditions and provides a robust framework for assessing erosion impacts on carbon (C) and nitrogen (N) cycling. Topsoil dilution consistently reduced CO_2 fluxes, with a significant decline observed only in the non-eroded LL soil, likely due to lower soil organic carbon (SOC) availability and potential C stabilization. In more eroded soils, this effect was weaker, probably because existing C undersaturation limited further mitigation. The response of N_2O emissions varied with soil properties; reductions occurred in the clay- and aluminium (Al) and iron (Fe) oxide-rich eLL soil, increases in calcareous RZ soil, and only minor increase in LL, likely due to reduced carbon-to-nitrogen ratio (C: N ratio). These results highlight that erosion state and soil properties strongly influence greenhouse gas (GHG) responses to digestate. Future research should test these processes under field conditions across different management and climatic settings and develop site-specific fertilization strategies tailored to local soil and erosion characteristics. In erosion-affected landscapes with high spatial variability, remote or proximal sensing can help identify key soil differences such as pH, texture, and organic matter content to adjust fertilizer application, improve nutrient efficiency, and minimize N_2O emissions.

Supplementary Information The online version contains supplementary material available at https://doi.org/10.1007/s42729-025-02940-9.

Acknowledgements This study was funded by German Federal Ministry of Food and Agriculture within the research project "Krumensenke" (Fachagentur fuer Nachwachsende Rohstoffe, FNR, BMEL) and by the German Research Foundation (Deutsche Forschungsgemeinschaft, DFG) within the research project "CropRhizoSOM".

Author Contributions Ayten Pehlivan wrote the manuscript in consultation with Mathias Hoffmann, Maire Holz, Maren Dubbert, Michael Sommer, and Jürgen Augustin. Jürgen Augustin was involved in designing the experiment and applying for funding. Steffen Kolb was involved in applying for funding. Jürgen Augustin supervised the experiment and Matthias Lück conducted the experiment. Ayten Pehlivan performed the data and statistical analyses in consultation with Mathias Hoffmann. All co-authors crosschecked the manuscript.

Funding Open Access funding enabled and organized by Projekt DEAL. This study was funded by the project 'Krumensenke' (Fachagentur fuer Nachwachsende Rohstoffe, FNR, BMEL) and the project 'CropRhizoSOM' (Deutsche Forschungsgemeinschaft, DFG; Project number 431061957).

Data Availability The datasets generated during and/or analysed during the current study are available in the BonaRes repository, [https://doi.org/10.4228/zalf-76tz-3k46]

Declarations

Ethical approval This manuscript has not been published elsewhere and is not under consideration by any other journal. Furthermore, there are no conflicts with the ethical responsibilities formulated by Springer (https://www.springer.com/journal/11104/submission-guidelines#Instructions for authors_Ethical Responsibilities of Authors).

Consent for publication All the authors have approved the submission of the manuscript to Journal of Soil Science and Plant Nutrition.

Consent to participate Not applicable (no human participants and/or animals).

Conflict of interest The authors declare they have no financial or non-financial conflicts of interest as described, e.g., by Springer (https://www.springer.com/journal/11104/submission-guidelines#Instructions for authors_Ethical Responsibilities of Authors).

References

Akiyama H, Yamamoto A, Uchida Y, Hoshino YT, Tago K, Wang Y, Hayatsu M (2020) Effect of low C/N crop residue input on N2O, NO, and CH4 fluxes from Andosol and Fluvisol fields. Sci Total Environ 713:136677. https://doi.org/10.1016/j.scitotenv.2020.136677

Alburquerque JA, de la Fuente C, Bernal MP (2012) Chemical properties of anaerobic digestates affecting C and N dynamics in amended soils. Agric Ecosyst Environ 160:15–22. https://doi.org/10.1016/j.agee.2011.03.007

Allison M, Ausden M (2004) Successful use of topsoil removal and soil amelioration to create heathland vegetation. Biol Conserv 120:221–228. https://doi.org/10.1016/j.biocon.2004.02.017

Baggs EM, Rees RM, Smith KA, Vinten AJA (2000) Nitrous oxide emission from soils after incorporating crop residues. Soil Use Manage 16:82–87. https://doi.org/10.1111/j.1475-2743.2000.tb00179.x

Baldock JA, Skjemstad JO (2000) Role of the soil matrix and minerals in protecting natural organic materials against biological attack. Org Geochem 31:697–710. https://doi.org/10.1016/S0146-6380(00)00049-8

Bateman EJ, Baggs EM (2005) Contributions of nitrification and denitrification to N2O emissions from soils at different water-filled pore space. Biol Fertil Soils 41:379–388. https://doi.org/10.1007/s00374-005-0858-3

Batlle-Aguilar J, Brovelli A, Porporato A, Barry DA (2011) Modelling soil carbon and nitrogen cycles during land use change. A review. Agron Sustain Dev 31:251–274. https://doi.org/10.1051/agro/2010007

Berhe AA, Kleber M (2013) Erosion, deposition, and the persistence of soil organic matter: mechanistic considerations and problems with terminology. Earth Surf Process Landforms 38:908–912. https://doi.org/10.1002/esp.3408

Berhe AA, Barnes RT, Six J, Marín-Spiotta E (2018) Role of soil erosion in biogeochemical cycling of essential elements: carbon, nitrogen, and phosphorus. Annu Rev Earth Planet Sci 46:521–548. https://doi.org/10.1146/annurev-earth-082517-010018

Bingham AH, Cotrufo MF (2016) Organic nitrogen storage in mineral soil: implications for policy and management. Sci Total Environ 551:116–126. https://doi.org/10.1016/j.scitotenv.2016.02.020

Bol R, Moering J, Kuzyakov Y, Amelung W (2003) Quantification of priming and CO2 respiration sources following slurry-C incorporation into two grassland soils with different C content. Rapid Commun Mass Spectrom 17:2585–2590. https://doi.org/10.1002/rcm.1184

Castellano MJ, Kaye JP, Lin H, Schmidt JP (2012) Linking carbon saturation concepts to nitrogen saturation and retention. Ecosystems 15:175–187. https://doi.org/10.1007/s10021-011-9501-3

Chen D, Li Y, Grace P, Mosier AR (2008) N2O emissions from agricultural lands: a synthesis of simulation approaches. Plant Soil 309:169–189. https://doi.org/10.1007/s11104-008-9634-0

Cui F, Yan G, Zhou Z, Zheng X, Deng J (2012) Annual emissions of nitrous oxide and nitric oxide from a wheat–maize cropping system on a silt loam calcareous soil in the North China Plain. Soil Biol Biochem 48:10–19. https://doi.org/10.1016/j.soilbio.2012.01.007

de la Fuente C, Alburquerque JA, Clemente R, Bernal MP (2013) Soil C and N mineralisation and agricultural value of the products of an anaerobic digestion system. Biol Fertil Soils 49:313–322. https://doi.org/10.1007/s00374-012-0719-9

Deumlich D, Rogasik H, Hierold W, Onasch I, Völker L, Sommer M (2017) The carboZALF-d manipulation experiment – experimental design and SOC patterns. Int J Environ Agric Res 3:40–50

Diacono M, Montemurro F (2011) Long-Term effects of organic amendments on soil fertility. In: Lichtfouse E, Hamelin M, Navarrete M, Debaeke P (eds) Sustainable agriculture volume 2. Springer Netherlands, Dordrecht, pp 761–786

Dialynas YG, Bras RL, deB Richter D (2017) Hydro-geomorphic perturbations on the soil-atmosphere CO2 exchange: how (un)certain are our balances? Water Resour Res 53:1664–1682. https://doi.org/10.1002/2016WR019411

Dietrich M, Fongen M, Foereid B (2020) Greenhouse gas emissions from digestate in soil. Int J Recycl Org Waste Agric 9:1–9. https://doi.org/10.30486/ijrowa.2020.1885341.1005

Dobbie KE, Smith KA (2003) Nitrous oxide emission factors for agricultural soils in great britain: the impact of soil water-filled pore space and other controlling variables. Glob Chang Biol 9:204–218. https://doi.org/10.1046/j.1365-2486.2003.00563.x

Doetterl S, Berhe AA, Nadeu E, Wang Z, Sommer M, Fiener P (2016) Erosion, deposition and soil carbon: a review of process-level controls, experimental tools and models to address C cycling in dynamic landscapes. Earth-Sci Rev 154:102–122. https://doi.org/10.1016/j.earscirev.2015.12.005

Doetterl S, Berhe AA, Heckman K, Lawrence C, Schnecker J, Vargas R, Vogel C, Wagai RA (2025) Landscape-scale view of soil organic matter dynamics. Nat Rev Earth Environ 6:67–81. https://doi.org/10.1038/s43017-024-00621-2

Fangueiro D, Chadwick D, Dixon L, Grilo J, Walter N, Bol R (2010) Short term N2O, CH4 and CO2 production from soil sampled at different depths and amended with a fine sized slurry fraction. Chemosphere 81:100–108. https://doi.org/10.1016/j.chemosphere.2010.06.049

Gao N, Yang B, Song Q, Li X, Chen W, Shen Y, Li S (2023) Ammonia-oxidizing bacteria-driven autotrophic nitrification dominated nitrous oxide production in calcareous soil under long term plastic film mulching. Geoderma 435:116523. https://doi.org/10.1016/j.geoderma.2023.116523

Geissen V, Wang S, Oostindie K, Huerta E, Zwart KB, Smit A, Moore D (2013) Effects of topsoil removal as a nature management technique on soil functions. CATENA 101:50–55. https://doi.org/10.1016/j.catena.2012.10.002

Georgiou K, Angers D, Champiny RE, Cotrufo MF, Craig ME, Doetterl S, Grandy AS, Lavallee JM, Lin Y, Lugato E, Poeplau C, Rocci KS, Schweizer SA, Six J, Wieder WR (2025) Soil carbon saturation: what do we really know? Glob Change Biol 31:e70197. https://doi.org/10.1111/gcb.70197

Gerke HH, Hierold W (2012) Vertical bulk density distribution in C-horizons from Marley till as indicator for erosion history in a hummocky post-glacial soil landscape. Soil Tillage Res 125:116–122. https://doi.org/10.1016/j.still.2012.06.005

Gerke HH, Rieckh H, Sommer M (2016) Interactions between crop, water, and dissolved organic and inorganic carbon in a hummocky landscape with erosion-affected pedogenesis. Soil Tillage Res 156:230–244. https://doi.org/10.1016/j.still.2015.09.003

Gregorich EG, Greer KJ, Anderson DW, Liang BC (1998) Carbon distribution and losses: erosion and deposition effects. Soil Tillage Res 47:291–302. https://doi.org/10.1016/S0167-1987(98)00117-2

Groffman PM, Boulware NJ, Zipperer WC, Pouyat RV, Band LE, Colosimo MF (2002) Soil nitrogen cycle processes in urban

riparian zones. Environ Sci Technol 36:4547–4552. https://doi.org/10.1021/es020649z
Gu J, Nicoullaud B, Rochette P, Pennock DJ, Hénault C, Cellier P, Richard G (2011) Effect of topography on nitrous oxide emissions from winter wheat fields in central France. Environ Pollut 159:3149–3155. https://doi.org/10.1016/j.envpol.2011.04.009
Harden JW, Sharpe JM, Parton WJ, Ojima DS, Fries TL, Huntington TG, Dabney SM (1999) Dynamic replacement and loss of soil carbon on eroding cropland. Glob Biogeochem Cycles 13:885–901. https://doi.org/10.1029/1999GB900061
Hassink J (1997) The capacity of soils to preserve organic C and N by their association with clay and silt particles. Plant Soil 191:77–87. https://doi.org/10.1023/A:1004213929699
Hassink J, Whitmore AP (1997) A model of the physical protection of organic matter in soils. Soil Sci Soc Am J 61:131–139. https://doi.org/10.2136/sssaj1997.03615995006100010020x
Hoffmann M, Jurisch N, Garcia Alba J, Albiac Borraz E, Schmidt M, Huth V, Augustin J (2017) Detecting small-scale spatial heterogeneity and temporal dynamics of soil organic carbon (SOC) stocks: a comparison between automatic chamber-derived C budgets and repeated soil inventories. Biogeosciences 14:1003–1019. https://doi.org/10.5194/bg-14-1003-2017
Hoffmann M, Pohl M, Jurisch N, Prescher AK, Mendez Campa E, Hagemann U, Augustin J (2018) Maize carbon dynamics are driven by soil erosion state and plant phenology rather than nitrogen fertilization form. Soil Tillage Res 175:255–266. https://doi.org/10.1016/j.still.2017.09.004
Holz M, Augustin J (2021) Erosion effects on soil carbon and nitrogen dynamics on cultivated slopes: a meta-analysis. Geoderma 397:115045. https://doi.org/10.1016/j.geoderma.2021.115045
Jäger N, Duffner A, Ludwig B, Flessa H (2013) Effect of fertilization history on short-term emission of CO2 and N2O after the application of different N fertilizers – a laboratory study. Arch Agron Soil Sci 59:161–171. https://doi.org/10.1080/03650340.2011.621420
Johansen A, Carter MS, Jensen ES, Hauggard-Nielsen H, Ambus P (2013) Effects of digestate from anaerobically digested cattle slurry and plant materials on soil microbial community and emission of CO2 and N2O. Appl Soil Ecol 63:36–44. https://doi.org/10.1016/j.apsoil.2012.09.003
Kaiser K, Guggenberger G (2003) Mineral surfaces and soil organic matter. Eur J Soil Sci 54:219–236. https://doi.org/10.1046/j.1365-2389.2003.00544.x
Knicker H (2011) Soil organic N - an under-rated player for C sequestration in soils? Soil Biol Biochem 43:1118–1129. https://doi.org/10.1016/j.soilbio.2011.02.020
Kögel-Knabner I, Guggenberger G, Kleber M, Kandeler E, Kalbitz K, Scheu S, Leinweber P (2008) Organo-mineral associations in temperate soils: integrating biology, mineralogy, and organic matter chemistry. J Plant Nutr Soil Sci 171:61–82. https://doi.org/10.1002/jpln.200700048
Kyveryga PM, Blackmer AM, Ellsworth JW, Isla R (2004) Soil pH effects on nitrification of fall-applied anhydrous ammonia. Soil Sci Soc Am J 68:545–551. https://doi.org/10.2136/sssaj2004.5450
Lal R (2019) Accelerated soil erosion as a source of atmospheric CO2. Soil Tillage Res 188:35–40. https://doi.org/10.1016/j.still.2018.02.001
Larney FJ, Angers DA (2012) The role of organic amendments in soil reclamation: a review. Can J Soil Sci 92:19–38. https://doi.org/10.4141/cjss2010-064
Larney FJ, Li L, Janzen HH, Angers DA, Olson BM (2016) Soil quality attributes, soil resilience, and legacy effects following topsoil removal and one-time amendments. Can J Soil Sci 96:177–190. https://doi.org/10.1139/cjss-2015-0089
Levavasseur F, Le Roux C, Kouakou P, Jean-Baptiste V, Houot S (2022) High nitrogen availability but limited potential carbon storage in anaerobic digestates from cover crops. J Soil Sci Plant Nutr 22:2891–2896. https://doi.org/10.1007/s42729-022-00853-5
Livingston GP, Hutchinson GL (1995) Enclosure-based measurement of trace gas exchange: applications and sources of error. In: Matson PA, Harris RC (eds) Biogenic trace gases: measuring emissions from soil and water. Blackwell Science Ltd., Oxford, UK, pp 14–51
Loubet B, Laville P, Lehuger S, Larmanou E, Fléchard C, Mascher N, Cellier P (2011) Carbon, nitrogen and greenhouse gases budgets over a four years crop rotation in Northern France. Plant Soil 343:109–137. https://doi.org/10.1007/s11104-011-0751-9
Lützow Mv, Kögel-Knabner I, Ekschmitt K, Matzner E, Guggenberger G, Marschner B, Flessa H (2006) Stabilization of organic matter in temperate soils: mechanisms and their relevance under different soil conditions – a review. Eur J Soil Sci 57:426–445. https://doi.org/10.1111/j.1365-2389.2006.00809.x
Ma Z, Li Q, Yue Q, Gao B, Li W, Xu X, Zhong Q (2011) Adsorption removal of ammonium and phosphate from water by fertilizer controlled release agent prepared from wheat straw. Chem Eng J 171:1209–1217. https://doi.org/10.1016/j.cej.2011.05.027
Möller K (2015) Effects of anaerobic digestion on soil carbon and nitrogen turnover, N emissions, and soil biological activity. A review. Agron Sustain Dev 35:1021–1041. https://doi.org/10.1007/s13593-015-0284-3
Niemeyer M, Niemeyer T, Fottner S, Härdtle W, Mohamed A (2007) Impact of sod-cutting and choppering on nutrient budgets of dry heathlands. Biol Conserv 134:344–353. https://doi.org/10.1016/j.biocon.2006.07.013
Nkoa R (2014) Agricultural benefits and environmental risks of soil fertilization with anaerobic digestates: a review. Agron Sustain Dev 34:473–492. https://doi.org/10.1007/s13593-013-0196-z
O'Connor J, Mickan BS, Rinklebe J, Song H, Siddique KHM, Wang H, Kirkham MB, Bolan NS (2022) Environmental implications, potential value, and future of food-waste anaerobic digestate management: a review. J Environ Manag 318:115519. https://doi.org/10.1016/j.jenvman.2022.115519
Pehlivan A, Ruggaber J, Remus R, Augustin J, Kolb S (2025) Impact of erosion-induced topsoil dilution on rapeseed root growth, assimilate C input, and turnover in the soil. J Soil Sci Plant Nutr. https://doi.org/10.1007/s42729-025-02405-z
Pennock DJ (1998) New perspectives on the soil erosion-soil quality relationship. Joint FAO/IAEA Division of Nuclear Techniques in Food and Agriculture, Vienna (Austria), IAEA
Pezzolla D, Bol R, Gigliotti G, Sawamoto T, López AL, Cardenas L, Chadwick D (2012) Greenhouse gas (GHG) emissions from soils amended with digestate derived from anaerobic treatment of food waste. Rapid Commun Mass Spectrom 26:2422–2430. https://doi.org/10.1002/rcm.6362
R-Core-Team (2022) R: a language and environment for statistical computing. R Foundation for Statistical Computing, Vienna
Rashmi I, Roy T, Kartika KS, Pal R, Coumar V, Kala S, Shinoji KC (2020) Organic and inorganic fertilizer contaminants in agriculture: impact on soil and water resources. In: Naeem M, Ansari AA, Gill SS (eds) Contaminants in agriculture: sources, impacts and management. Springer International Publishing, Cham, pp 3–41
Remus R, Kaiser M, Kleber M, Augustin J, Sommer M (2018) Demonstration of the rapid incorporation of carbon into protective, mineral-associated organic carbon fractions in an eroded soil from the CarboZALF experimental site. Plant Soil 430:329–348. https://doi.org/10.1007/s11104-018-3724-4
Reuland G, Sigurnjak I, Dekker H, Sleutel S, Meers E (2022) Assessment of the carbon and nitrogen mineralisation of digestates elaborated from distinct feedstock profiles. Agronomy 12:456. https://doi.org/10.3390/agronomy12020456

Revuelta-Aramburu M, Santos-Montes AM, Morales-Polo C (2025) A review on anaerobic digestate as a biofertilizer: characteristics, production, and environmental impacts from a life cycle assessment perspective. Appl Sci 15:8635. https://doi.org/10.3390/app15158635

Rieckh H, Gerke HH, Sommer M (2012) Hydraulic properties of characteristic horizons depending on relief position and structure in a hummocky glacial soil landscape. Soil Tillage Res 125:123–131. https://doi.org/10.1016/j.still.2012.07.004

Rillig MC, Caldwell BA, Wösten HAB, Sollins P (2007) Role of proteins in soil carbon and nitrogen storage: controls on persistence. Biogeochemistry 85:25–44. https://doi.org/10.1007/s10533-007-9102-6

Rillig MC, Hoffmann M, Lehmann A, Liang Y, Lück M, Augustin J (2021) Microplastic fibers affect dynamics and intensity of CO2 and N2O fluxes from soil differently. Microplastics Nanoplastics 1:3. https://doi.org/10.1186/s43591-021-00004-0

Rochette P, Angers DA, Côté D (2000) Soil carbon and nitrogen dynamics following application of pig slurry for the 19th consecutive year I. carbon dioxide fluxes and microbial biomass carbon. Soil Sci Soc Am J 64:1389–1395. https://doi.org/10.2136/sssaj2000.6441389x

Rosace MC, Veronesi F, Briggs S, Cardenas LM, Jeffery S (2020) Legacy effects override soil properties for CO2 and N2O but not CH4 emissions following digestate application to soil. GCB Bioenergy 12:445–457. https://doi.org/10.1111/gcbb.12688

Ruggaber J, Pehlivan A, Remus R, Francioli D, Wirth S, Augustin J, Kolb S (2024) Simulated soil erosion predominantly affects fungal abundance in the rapeseed rhizosphere. Rhizosphere 30:100912. https://doi.org/10.1016/j.rhisph.2024.100912

Sahrawat KL (2008) Factors affecting nitrification in soils. Commun Soil Sci Plant Anal 39:1436–1446. https://doi.org/10.1080/00103620802004235

Schlichting E, Blume HP, Stahr K (1995) Soils practical (in German). Blackwell, Berlin

Schoof J, Holz M, Rütting T, Well R, Buchen-Tschiskale C (2025) Impact of different soil erosion levels on gross N transformation processes and gaseous N losses: an incubation study. Soil Biol Biochem 209:109905. https://doi.org/10.1016/j.soilbio.2025.109905

Smith P, Martino D, Cai Z, Gwary D, Janzen H, Kumar P, Smith J (2008) Greenhouse gas mitigation in agriculture. Philos Trans R Soc Lond B Biol Sci 363:789–813. https://doi.org/10.1098/rstb.2007.2184

Sollins P, Kramer MG, Swanston C, Lajtha K, Filley T, Aufdenkampe AK, Bowden RD (2009) Sequential density fractionation across soils of contrasting mineralogy: evidence for both microbial- and mineral-controlled soil organic matter stabilization. Biogeochemistry 96:209–231. https://doi.org/10.1007/s10533-009-9359-z

Sommer M, Gerke HH, Deumlich D (2008) Modelling soil landscape genesis — a time split approach for hummocky agricultural landscapes. Geoderma 145:480–493. https://doi.org/10.1016/j.geoderma.2008.01.012

Sommer M, Augustin J, Kleber M (2016) Feedbacks of soil erosion on SOC patterns and carbon dynamics in agricultural landscapes—the CarboZALF experiment. Soil Tillage Res 156:182–184. https://doi.org/10.1016/j.still.2015.09.015

Spielvogel S, Prietzel J, Kögel-Knabner I (2008) Soil organic matter stabilization in acidic forest soils is preferential and soil type-specific. Eur J Soil Sci 59:674–692. https://doi.org/10.1111/j.1365-2389.2008.01030.x

Stewart CE, Paustian K, Conant RT, Plante AF, Six J (2007) Soil carbon saturation: concept, evidence and evaluation. Biogeochemistry 86:19–31. https://doi.org/10.1007/s10533-007-9140-0

Stewart CE, Paustian K, Conant RT, Plante AF, Six J (2009) Soil carbon saturation: implications for measurable carbon pool dynamics in long-term incubations. Soil Biol Biochem 41:357–366. https://doi.org/10.1016/j.soilbio.2008.11.011

Tao R, Wakelin SA, Liang Y, Chu G (2017) Response of ammonia-oxidizing archaea and bacteria in calcareous soil to mineral and organic fertilizer application and their relative contribution to nitrification. Soil Biol Biochem 114:20–30. https://doi.org/10.1016/j.soilbio.2017.06.027

Vaidya S, Schmidt M, Rakowski P, Bonk N, Verch G, Augustin J, Hoffmann M (2021) A novel robotic chamber system allowing to accurately and precisely determining spatio-temporal CO2 flux dynamics of heterogeneous croplands. Agric For Meteorol 296:108206. https://doi.org/10.1016/j.agrformet.2020.108206

Vaidya S, Hoffmann M, Holz M, Macagga R, Monzon O, Thalmann M, Augustin J (2023) Similar strong impact of N fertilizer form and soil erosion state on N2O emissions from croplands. Geoderma 429:116243. https://doi.org/10.1016/j.geoderma.2022.116243

Vaidya S, Hoffmann M, Dubbert M, Kramp K, Schmidt M, Verch G, Augustin J (2024) Topsoil dilution by subsoil admixture had less impact on soil organic carbon stock development than fertilizer form and erosion state. Sci Total Environ 946:174243. https://doi.org/10.1016/j.scitotenv.2024.174243

van Groenigen JW, Huygens D, Boeckx P, Kuyper TW, Lubbers IM, Rütting T, Groffman PM (2015) The soil N cycle: new insights and key challenges. Soil 1:235–256. https://doi.org/10.5194/soil-1-235-2015

Vilain G, Garnier J, Tallec G, Cellier P (2010) Effect of slope position and land use on nitrous oxide (N2O) emissions (Seine Basin, France). Agric For Meteorol 150:1192–1202. https://doi.org/10.1016/j.agrformet.2010.05.004

Vogel C, Mueller CW, Höschen C, Buegger F, Heister K, Schulz S, Kögel-Knabner I (2014) Submicron structures provide preferential spots for carbon and nitrogen sequestration in soils. Nat Commun 5:2947. https://doi.org/10.1038/ncomms3947

Vogel C, Heister K, Buegger F, Tanuwidjaja I, Haug S, Schloter M, Kögel-Knabner I (2015) Clay mineral composition modifies decomposition and sequestration of organic carbon and nitrogen in fine soil fractions. Biol Fertil Soils 51:427–442. https://doi.org/10.1007/s00374-014-0987-7

Wang X, Lü S, Gao C, Xu X, Zhang X, Bai X, Wu L (2014) Highly efficient adsorption of ammonium onto Palygorskite nanocomposite and evaluation of its recovery as a multifunctional slow-release fertilizer. Chem Eng J 252:404–414. https://doi.org/10.1016/j.cej.2014.04.097

West TO, Six J (2007) Considering the influence of sequestration duration and carbon saturation on estimates of soil carbon capacity. Clim Change 80:25–41. https://doi.org/10.1007/s10584-006-9173-8

Wilken F, Ketterer M, Koszinski S, Sommer M, Fiener P (2020) Understanding the role of water and tillage erosion from 239+240Pu tracer measurements using inverse modelling. SOIL 6:549–564. https://doi.org/10.5194/soil-6-549-2020

Xiao H, Li Z, Chang X, Huang B, Nie X, Liu C, Jiang J (2018) The mineralization and sequestration of organic carbon in relation to agricultural soil erosion. Geoderma 329:73–81. https://doi.org/10.1016/j.geoderma.2018.05.018

Yao Z, Yan G, Ma L, Wang Y, Zhang H, Zheng X, Butterbach-Bahl K (2022) Soil C/N ratio is the dominant control of annual N2O fluxes from organic soils of natural and semi-natural ecosystems. Agric For Meteorol 327:109198. https://doi.org/10.1016/j.agrformet.2022.109198

Yu WH, Li N, Tong DS, Zhou CH, Lin CX, Xu CY (2013) Adsorption of proteins and nucleic acids on clay minerals and their

interactions: a review. Appl Clay Sci 80:443–452. https://doi.org/10.1016/j.clay.2013.06.003

Zentgraf I, Hoffmann M, Augustin J, Buchen-Tschiskale C, Hoferer S, Holz M (2024) Effect of mineral and organic fertilizer on N dynamics upon erosion-induced topsoil dilution. Heliyon. https://doi.org/10.1016/j.heliyon.2024.e34822

Zhang J, Zhu T, Cai Z, Qin S, Müller C (2012) Effects of long-term repeated mineral and organic fertilizer applications on soil nitrogen transformations. Eur J Soil Sci 63:75–85. https://doi.org/10.1111/j.1365-2389.2011.01410.x

Zhang D, Zhang H, Xie J, Sun Y, Zhu J, Wang D (2024) A critical review on sustainable management and resource utilization of digestate. Process Saf Environ Prot 183:339–354. https://doi.org/10.1016/j.psep.2024.01.029